

## Chapter 11

# Qualitative dynamics, for pedestrians

The classification of the constituents of a chaos, nothing less is here essayed.

Herman Melville, *Moby Dick*, chapter 32

In this chapter we begin to learn how to use qualitative properties of a flow in order to *partition* the phase space in a topologically invariant way, and *name* topologically distinct orbits. This will enable us – in chapter 13 – to *count* the distinct orbits, and in the process touch upon all the main themes of this book, going the whole distance from diagnosing chaotic dynamics to computing zeta functions.

We start by a simple physical example, symbolic dynamics of a 3-disk game of pinball, and then show that also for smooth flows the qualitative dynamics of stretching and folding flows enables us to partition the phase space and assign symbolic dynamics itineraries to trajectories. Here we illustrate the method on a  $1-d$  approximation to Rössler flow. In chapter 13 we turn this topological dynamics into a multiplicative operation on the phase space partitions by means of transition matrices/Markov graphs, the simplest examples of evolution operators. Deceptively simple, this subject can get very difficult very quickly, so in this chapter we do the first pass, at a pedestrian level, postponing the discussion of higher-dimensional, cyclist level issues to chapter 12.

Even though by inclination you might only care about the serious stuff, like Rydberg atoms or mesoscopic devices, and resent wasting time on things formal, this chapter and chapter 13 are good for you. Read them.

### 11.1 Qualitative dynamics

(R. Mainieri and P. Cvitanović)

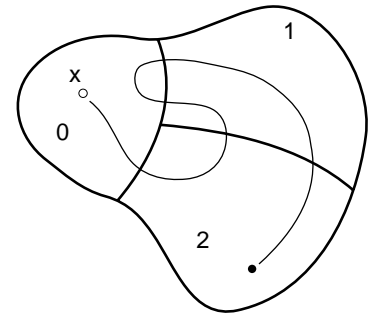


**Figure 11.1:** A trajectory with itinerary 021012.

What can a flow do to the phase space points? This is a very difficult question to answer because we have assumed very little about the evolution function  $f^t$ ; continuity, and differentiability a sufficient number of times. Trying to make sense of this question is one of the basic concerns in the study of dynamical systems. One of the first answers was inspired by the motion of the planets: they appear to repeat their motion through the firmament. Motivated by this observation, the first attempts to describe dynamical systems were to think of them as periodic.

However, periodicity is almost never quite exact. What one tends to observe is *recurrence*. A recurrence of a point  $x_0$  of a dynamical system is a return of that point to a neighborhood of where it started. How close the point  $x_0$  must return is up to us: we can choose a volume of any size and shape, and call it the neighborhood  $\mathcal{M}_0$ , as long as it encloses  $x_0$ . For chaotic dynamical systems, the evolution might bring the point back to the starting neighborhood infinitely often. That is, the set

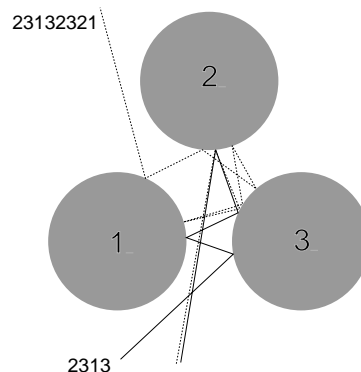
$$\{y \in \mathcal{M}_0 : y = f^t(x_0), t > t_0\} \quad (11.1)$$

will in general have an infinity of recurrent episodes.

To observe a recurrence we must look at neighborhoods of points. This suggests another way of describing how points move in phase space, which turns out to be the important first step on the way to a theory of dynamical systems: qualitative, topological dynamics, or, as it is usually called, *symbolic dynamics*. As the subject can get quite technical, a summary of the basic notions and definitions of symbolic dynamics is relegated to sect. 11.6; check that section whenever you run into obscure symbolic dynamics jargon.

We start by cutting up the phase space up into regions  $\mathcal{M}_A, \mathcal{M}_B, \dots, \mathcal{M}_Z$ . This can be done in many ways, not all equally clever. Any such division of the phase space into topologically distinct regions is a *partition*, and we associate with each region (sometimes referred to as a *state*) a symbol  $s$  from an  $N$ -letter *alphabet* or *state set*  $\mathcal{A} = \{A, B, C, \dots, Z\}$ . As the dynamics moves the point through the phase space, different regions will be visited. The visitation sequence - forthwith referred to as the *itinerary* - can be represented by the letters of the alphabet  $\mathcal{A}$ . If, as in the example sketched in figure 11.1, the phase space is divided into three regions  $\mathcal{M}_0$ ,

**Figure 11.2:** Two pinballs that start out very close to each other exhibit the same qualitative dynamics  $\_2313\_$  for the first three bounces, but due to the exponentially growing separation of trajectories with time, follow different itineraries thereafter: one escapes after  $\_2313\_$ , the other one escapes after  $\_23132321\_$



$\mathcal{M}_1$ , and  $\mathcal{M}_2$ , the “letters” are the integers  $\{0, 1, 2\}$ , and the itinerary for the trajectory sketched in the figure is  $0 \mapsto 2 \mapsto 1 \mapsto 0 \mapsto 1 \mapsto 2 \mapsto \dots$ .

If there is no way to reach partition  $\mathcal{M}_i$  from partition  $\mathcal{M}_j$ , and conversely, partition  $\mathcal{M}_j$  from partition  $\mathcal{M}_i$ , the phase space consists of at least two disconnected pieces, and we can analyze it piece by piece. An interesting partition should be dynamically connected, i.e., one should be able to go from any region  $\mathcal{M}_i$  to any other region  $\mathcal{M}_j$  in a finite number of steps. A dynamical system with such partition is said to be *metrically indecomposable*.

In general one also encounters transient regions - regions to which the dynamics does not return to once they are exited. Hence we have to distinguish between (for us uninteresting) wandering trajectories that never return to the initial neighborhood, and the non-wandering set (2.2) of the *recurrent* trajectories.

The allowed transitions between the regions of a partition are encoded in the  $[N \times N]$ -dimensional *transition matrix* whose elements take values

$$T_{ij} = \begin{cases} 1 & \text{if a transition } \mathcal{M}_j \rightarrow \mathcal{M}_i \text{ is possible} \\ 0 & \text{otherwise.} \end{cases} \quad (11.2)$$

The transition matrix encodes the topological dynamics as an invariant law of motion, with the allowed transitions at any instant independent of the trajectory history, requiring no memory.

**Example 11.1 Complete  $N$ -ary dynamics:** *All transition matrix entries equal unity (one can reach any region from any other region in one step):*

$$T_c = \begin{pmatrix} 1 & 1 & \dots & 1 \\ 1 & 1 & \dots & 1 \\ \vdots & \vdots & \ddots & \vdots \\ 1 & 1 & \dots & 1 \end{pmatrix}. \quad (11.3)$$

*Further examples of transition matrices, such as the 3-disk transition matrix (11.5) and the 1-step memory sparse matrix (11.15), are peppered throughout the text.*

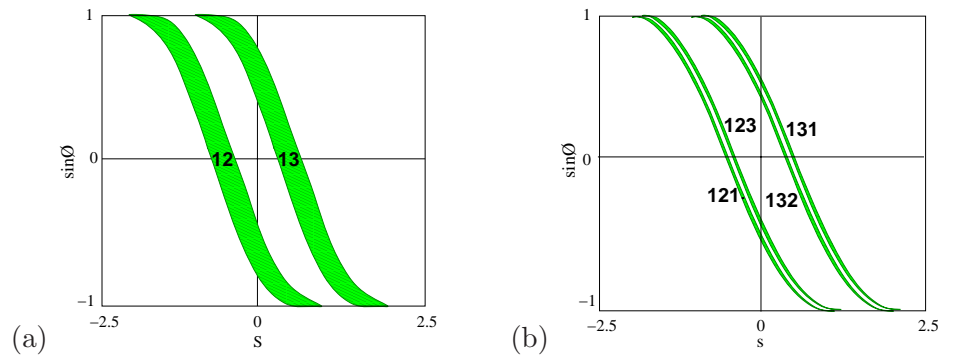


**Figure 11.3:** The 3-disk game of pinball Poincaré section, trajectories emanating from the disk 1 with  $x_0 = (\text{arclength, parallel momentum}) = (s_0, p_0)$ , disk radius : center separation ratio  $a:R = 1:2.5$ . (a) Strips of initial points  $\mathcal{M}_{12}$ ,  $\mathcal{M}_{13}$  which reach disks 2, 3 in one bounce, respectively. (b) Strips of initial points  $\mathcal{M}_{121}$ ,  $\mathcal{M}_{131}$ ,  $\mathcal{M}_{132}$  and  $\mathcal{M}_{123}$  which reach disks 1, 2, 3 in two bounces, respectively. (Y. Lan)

However, knowing that a point from  $\mathcal{M}_i$  reaches  $\mathcal{M}_j$  in one step is not quite good enough. We would be happier if we knew that *any* point in  $\mathcal{M}_i$  reaches  $\mathcal{M}_j$ ; otherwise we have to subpartition  $\mathcal{M}_i$  into the points which land in  $\mathcal{M}_j$ , and those which do not, and often we will find ourselves partitioning *ad infinitum*.

Such considerations motivate the notion of a *Markov partition*, a partition for which no memory of preceding steps is required to fix the transitions allowed in the next step. Dynamically, *finite Markov partitions* can be generated by *expanding*  $d$ -dimensional iterated mappings  $f : \mathcal{M} \rightarrow \mathcal{M}$ , if  $\mathcal{M}$  can be divided into  $N$  regions  $\{\mathcal{M}_0, \mathcal{M}_1, \dots, \mathcal{M}_{N-1}\}$  such that in one step points from an initial region  $\mathcal{M}_i$  either fully cover a region  $\mathcal{M}_j$ , or miss it altogether,

$$\text{either } \mathcal{M}_j \cap f(\mathcal{M}_i) = \emptyset \quad \text{or} \quad \mathcal{M}_j \subset f(\mathcal{M}_i). \quad (11.4)$$

Let us illustrate what this means by our favorite example, the game of pinball.

**Example 11.2 3-disk symbolic dynamics:** Consider the motion of a free point particle in a plane with 3 elastically reflecting convex disks. After a collision with a disk a particle either continues to another disk or escapes, and any trajectory can be labeled by the disk sequence. For example, if we label the three disks by 1, 2 and 3, the two trajectories in figure 11.2 have itineraries  $\_2313\_$ ,  $\_23132321\_$  respectively. The 3-disk prime cycles given in figures 1.6 and 11.6 are further examples of such itineraries.

At each bounce a cone of initially nearby trajectories defocuses (see figure 1.8), and in order to attain a desired longer and longer itinerary of bounces the initial point  $x_0 = (s_0, p_0)$  has to be specified with a larger and larger precision, and lie within initial phase space strips drawn in figure 11.3. Similarly, it is intuitively clear that as we go backward in time (in this case, simply reverse the velocity vector), we also need increasingly precise specification of  $x_0 = (s_0, p_0)$  in order to follow a given past itinerary. Another way to look at the survivors after two bounces is to plot  $\mathcal{M}_{s_1, s_2}$ , the intersection of  $\mathcal{M}_{s_2}$  with the strips  $\mathcal{M}_{s_1}$ , obtained by time reversal (the velocity

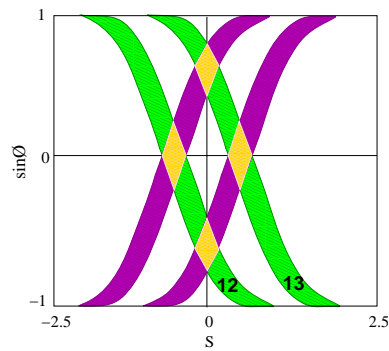


**Figure 11.4:** The Poincaré section of the phase space for the binary labeled pinball. For definitiveness, this set is generated by starting from disk 1, preceded by disk 2. Indicated are the fixed points  $\bar{0}$ ,  $\bar{1}$  and the 2-cycle periodic points  $\bar{01}$ ,  $\bar{10}$ , together with strips which survive 1, 2, ... bounces. Iteration corresponds to the decimal point shift; for example, all points in the rectangle  $[01.01]$  map into the rectangle  $[010.1]$  in one iteration. See also figure 11.6 (b).

changes sign  $\sin \phi \rightarrow -\sin \phi$ ).  $\mathcal{M}_{s_1, s_2}$ , figure 11.4, is a “rectangle” of nearby trajectories which have arrived from the disk  $s_1$  and are heading for the disk  $s_2$ .

We see that a finite length trajectory is not uniquely specified by its finite itinerary, but an isolated unstable cycle is: its itinerary is an infinitely repeating block of symbols. More generally, for hyperbolic flows the intersection of the future and past itineraries, the bi-infinite itinerary  $S^- \cdot S^+ = \cdots s_{-2}s_{-1}s_0.s_1s_2s_3 \cdots$  specifies a unique trajectory. This is intuitively clear for our 3-disk game of pinball, and is stated more formally in the definition (11.4) of a Markov partition. The definition requires that the dynamics be expanding forward in time in order to ensure that the cone of trajectories with a given itinerary becomes sharper and sharper as the number of specified symbols is increased.

**Example 11.3 Pruning rules for a 3-disk alphabet:** *As the disks are convex, there can be no two consecutive reflections off the same disk, hence the covering symbolic dynamics consists of all sequences which include no symbol repetitions  $\_11\_$ ,  $\_22\_$ ,  $\_33\_$ . This is a finite set of finite length pruning rules, hence, the dynamics is a subshift of finite type (see (11.24) for definition), with the transition matrix (11.2) given by*

$$T = \begin{pmatrix} 0 & 1 & 1 \\ 1 & 0 & 1 \\ 1 & 1 & 0 \end{pmatrix}. \quad (11.5)$$

*For convex disks the separation between nearby trajectories increases at every reflection, implying that the stability matrix has an expanding eigenvalue. By the Liouville phase-space volume conservation (5.23), the other transverse eigenvalue is contracting. This example demonstrates that finite Markov partitions can be constructed for hyperbolic dynamical systems which are expanding in some directions, contracting in others. Further examples are the 1-dimensional expanding mapping sketched in figure 11.8, and more examples are worked out in sect. 23.2.*

Determining whether the symbolic dynamics is complete (as is the case for sufficiently separated disks), pruned (for example, for touching or over-

**Figure 11.5:** Binary labeling of the 3-disk pinball trajectories; a bounce in which the trajectory returns to the preceding disk is labeled 0, and a bounce which results in continuation to the third disk is labeled 1.



lapping disks), or only a first coarse graining of the topology (as, for example, for smooth potentials with islands of stability) requires case-by-case investigation, a discussion we postpone to sect. 11.4 and chapter 12. For the time being we assume that the disks are sufficiently separated that there is no additional pruning beyond the prohibition of self-bounces.



fast track:  
sect. 11.3, p. 166

## 11.2 A brief detour; recoding, symmetries, tilings



Though a useful tool, Markov partitioning is not without drawbacks. One glaring shortcoming is that Markov partitions are not unique: any of many different partitions might do the job. The 3-disk system offers a simple illustration of different Markov partitioning strategies for the same dynamical system.

The  $\mathcal{A} = \{1, 2, 3\}$  symbolic dynamics for 3-disk system is neither unique, nor necessarily the smartest one - before proceeding it pays to exploit the symmetries of the pinball in order to obtain a more efficient description. In chapter 22 we shall be handsomely rewarded for our labors.

As the three disks are equidistantly spaced, our game of pinball has a sixfold symmetry. For instance, the cycles  $\overline{12}$ ,  $\overline{23}$ , and  $\overline{13}$  are related to each other by rotation by  $\pm 2\pi/3$  or, equivalently, by a relabeling of the disks. Further examples of such symmetries are shown in figure 1.6. The disk labels are arbitrary; what is important is how a trajectory evolves as it hits subsequent disks, not what label the starting disk had. We exploit this symmetry by *recoding*, in this case replacing the absolute disk labels by relative symbols, indicating the type of the collision. For the 3-disk game of pinball there are two topologically distinct kinds of collisions, figure 11.5:

 11.1  
page 182

 11.2  
page 182

$$s_i = \begin{cases} 0 & : \quad \text{pinball returns to the disk it came from} \\ 1 & : \quad \text{pinball continues to the third disk.} \end{cases} \quad (11.6)$$

This *binary* symbolic dynamics has two immediate advantages over the ternary one; the prohibition of self-bounces is automatic, and the coding utilizes the symmetry of the 3-disk pinball game in elegant manner. If the disks are sufficiently far apart there are no further restrictions on symbols,

$n_p$	$p$	$n_p$	$p$	$n_p$	$p$	$n_p$	$p$	$n_p$	$p$
1	0	7	0001001	8	00001111	9	000001101	9	001001111
	1		0000111		00010111		000010011		001010111
2	01		0001011		00011011		000010101		001011011
3	001		0001101		00011101		000011001		001011101
	011		0010011		00100111		000100011		001100111
4	0001		0010101		00101011		000100101		001101011
	0011		0001111		00101101		000101001		001101101
	0111		0010111		00110101		000001111		001110101
5	00001		0011011		00011111		000010111		010101011
	00011		0011101		00101111		000011011		000111111
	00101	0101011	00110111	000011101	001011111				
	00111	0011111	00111011	000100111	001101111				
	01011	0101111	00111101	000101011	001110111				
	01111	0110111	01010111	000101101	001111011				
6	000001	0111111	01011011	000110011	001111101				
	000011	8	00000001	00111111	000110101	010101111			
	000101		00000011	01011111	000111001	010110111			
	000111		00000101	01101111	001001011	010111011			
	001011		00001001	01111111	001001101	001111111			
	001101		00000111	9	000000001	001010011	010111111		
	001111		00001011		000000011	001010101	011011111		
	010111		00001101		000000101	000011111	011101111		
	011111		00010011		000001001	000101111	011111111		
	7		0000001		00010101	000010001	000110111		
0000011			000111001		000000111	000111011			
0000101		00100101	000001011	000111101					
		00100101	000001011	000111101					

**Table 11.1:** Prime cycles for the binary symbolic dynamics up to length 9.

the symbolic dynamics is complete, and *all* binary sequences are admissible itineraries. As this type of symbolic dynamics pops up frequently, we list the shortest binary prime cycles in table 11.1.

 11.3  
page 182

**Example 11.4 Recoding ternary symbolic dynamics in binary:** Given a ternary sequence and labels of 2 preceding disks, rule (11.6) fixes the subsequent binary symbols. Here we list an arbitrary ternary itinerary, and the corresponding binary sequence:

$$\begin{array}{l}
 \text{ternary} : 3 \ 1 \ 2 \ 1 \ 3 \ 1 \ 2 \ 3 \ 2 \ 1 \ 2 \ 3 \ 1 \ 3 \ 2 \ 3 \\
 \text{binary} : \quad \cdot \ 1 \ 0 \ 1 \ 0 \ 1 \ 1 \ 0 \ 1 \ 0 \ 1 \ 1 \ 0 \ 1 \ 0
 \end{array} \tag{11.7}$$

The first 2 disks initialize the trajectory and its direction;  $3 \mapsto 1 \mapsto 2 \mapsto \dots$ . Due to the 3-disk symmetry the six 3-disk sequences initialized by 12, 13, 21, 23, 31, 32 respectively have the same weights, the same size partitions, and are coded by a single binary sequence. For periodic orbits, the equivalent ternary cycles reduce to binary cycles of  $1/3$ ,  $1/2$  or the same length. How this works is best understood by inspection of table 11.2, figure 11.6 and figure 22.3.

The 3-disk game of pinball is tiled by six copies of the *fundamental domain*, a one-sixth slice of the full 3-disk system, with the symmetry axes acting as reflecting mirrors, see figure 11.6 (b). Every global 3-disk trajectory has a corresponding fundamental domain mirror trajectory obtained by replacing every crossing of a symmetry axis by a reflection. Depending on the symmetry of the global trajectory, a repeating binary symbols block corresponds either to the full periodic orbit or to an irreducible segment

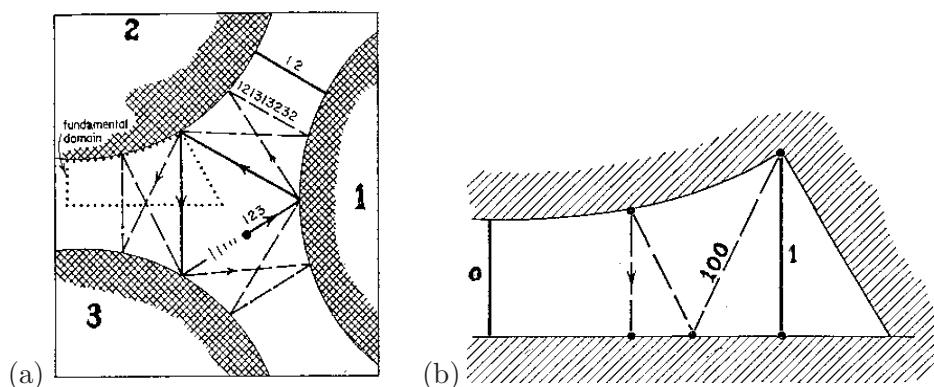


**Figure 11.6:** The 3-disk game of pinball with the disk radius : center separation ratio  $a:R = 1:2.5$ . (a) The three disks, with  $\overline{12}$ ,  $\overline{123}$  and  $\overline{1213232}$  cycles indicated. (b) The fundamental domain, i.e., the small  $1/6$ th wedge indicated in (a), consisting of a section of a disk, two segments of symmetry axes acting as straight mirror walls, and an escape gap. The above cycles restricted to the fundamental domain are now the two fixed points  $\overline{0}$ ,  $\overline{1}$ , and the  $\overline{100}$  cycle.

(examples are shown in figure 11.6 and table 11.2). An irreducible segment corresponds to a periodic orbit in the fundamental domain. Table 11.2 lists some of the shortest binary periodic orbits, together with the corresponding full 3-disk symbol sequences and orbit symmetries. For a number of reasons that will be elucidated in chapter 22, life is much simpler in the fundamental domain than in the full system, so whenever possible our computations will be carried out in the fundamental domain.

 11.5  
page 182

Inspecting the figure 11.3 we see that the relative ordering of regions with differing finite itineraries is a qualitative, topological property of the flow, so it makes sense to define a simple “canonical” representative partition which in a simple manner exhibits spatial ordering common to an entire class of topologically similar nonlinear flows.



in depth:  
chapter 22, p. 387

## 11.3 Stretch and fold

Symbolic dynamics for  $N$ -disk game of pinball is so straightforward that one may altogether fail to see the connection between the topology of hyperbolic flows and their symbolic dynamics. This is brought out more clearly by the 1-dimensional visualization of “stretch & fold” flows to which we turn now.

Suppose concentrations of certain chemical reactants worry you, or the variations in the Chicago temperature, humidity, pressure and winds affect your mood. All such properties vary within some fixed range, and so do their rates of change. Even if we are studying an open system such as the

$\tilde{p}$	$p$	$\mathfrak{g}_{\tilde{p}}$	$\tilde{p}$	$p$	$\mathfrak{g}_{\tilde{p}}$
0	1 2	$\sigma_{12}$	000001	121212 131313	$\sigma_{23}$
1	1 2 3	$C_3$	000011	121212 313131 232323	$C_3^2$
01	12 13	$\sigma_{23}$	000101	121213	$e$
001	121 232 313	$C_3$	000111	121213 212123	$\sigma_{12}$
011	121 323	$\sigma_{13}$	001011	121232 131323	$\sigma_{23}$
0001	1212 1313	$\sigma_{23}$	001101	121231 323213	$\sigma_{13}$
0011	1212 3131 2323	$C_3^2$	001111	121231 232312 313123	$C_3$
0111	1213 2123	$\sigma_{12}$	010111	121312 313231 232123	$C_3^2$
00001	12121 23232 31313	$C_3$	011111	121321 323123	$\sigma_{13}$
00011	12121 32323	$\sigma_{13}$	0000001	1212121 2323232 3131313	$C_3$
00101	12123 21213	$\sigma_{12}$	0000011	1212121 3232323	$\sigma_{13}$
00111	12123	$e$	0000101	1212123 2121213	$\sigma_{12}$
01011	12131 23212 31323	$C_3$	0000111	1212123	$e$
01111	12132 13123	$\sigma_{23}$	...	...	...

**Table 11.2:**  $C_{3v}$  correspondence between the binary labeled fundamental domain prime cycles  $\tilde{p}$  and the full 3-disk ternary labeled cycles  $p$ , together with the  $C_{3v}$  transformation that maps the end point of the  $\tilde{p}$  cycle into the irreducible segment of the  $p$  cycle, see sect. 22.2.2. Breaks in the ternary sequences mark repeats of the irreducible segment. The degeneracy of  $p$  cycle is  $m_p = 6n_{\tilde{p}}/n_p$ . The shortest pair of the fundamental domain cycles related by time reversal (but no spatial symmetry) are the 6-cycles  $\overline{001011}$  and  $\overline{001101}$ .

3-disk pinball game, we tend to be interested in a finite region around the disks and ignore the escapees. So a typical dynamical system that we care about is *bounded*. If the price for keeping going is high - for example, we try to stir up some tar, and observe it come to a dead stop the moment we cease our labors - the dynamics tends to settle into a simple limiting state. However, as the resistance to change decreases - the tar is heated up and we are more vigorous in our stirring - the dynamics becomes unstable.

If a flow is locally unstable but globally bounded, any open ball of initial points will be stretched out and then folded back.

At this juncture we show how this works on the simplest example: unimodal mappings of the interval. The erudite reader should skim through this chapter and then take a more demanding path, via the Smale horseshoes of chapter 12. Unimodal maps are easier, but physically less motivated. The Smale horseshoes are the high road, more complicated, but the right tool to generalize what we learned from the 3-disk dynamics, and begin analysis of general dynamical systems. It is up to you - unimodal maps suffice to get quickly to the heart of this treatise.

### 11.3.1 Temporal ordering: itineraries

In this section we learn how to *name* (and, in chapter 13, how to *count*) periodic orbits for the simplest, and nevertheless very instructive case, for 1-dimensional maps of an interval.

Suppose that the compression of the folded interval in figure 11.7 is so fierce that we can neglect the thickness of the attractor. For example, the

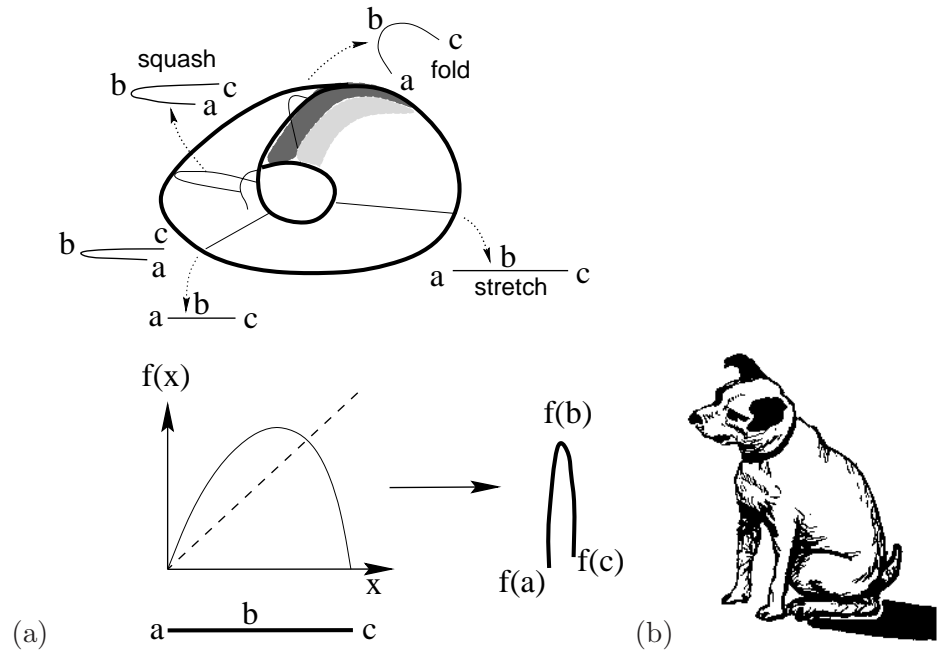


**Figure 11.7:** (a) A recurrent flow that stretches and folds. (b) The “stretch & fold” return map on the Poincaré section.

Rössler flow (2.14) is volume contracting, and an interval transverse to the attractor is stretched, folded and pressed back into a nearly 1-dimensional interval, typically compressed transversally by a factor of  $\approx 10^{13}$  in one Poincaré section return. In such cases it makes sense to approximate the return map of a “stretch & fold” flow by a 1-dimensional map.

The simplest mapping of this type is *unimodal*; interval is stretched and folded only once, with at most two points mapping into a point in the refolded interval. A unimodal map  $f(x)$  is a 1-dimensional function  $\mathbb{R} \rightarrow \mathbb{R}$  defined on an interval  $\mathcal{M} \in \mathbb{R}$  with a monotonically increasing (or decreasing) branch, a *critical point* (or interval)  $x_c$  for which  $f(x_c)$  attains the maximum (minimum) value, followed by a monotonically decreasing (increasing) branch. *Uni*-modal means that the map is a one-humped map with one critical point within interval  $\mathcal{M}$ . A *multi*-modal map has several critical points within interval  $\mathcal{M}$ .

**Example 11.5 Complete tent map, logistic map:** *The simplest examples of unimodal maps are the complete tent map, figure 11.8 (a),*

$$f(\gamma) = 1 - 2|\gamma - 1/2|, \tag{11.8}$$

*and the quadratic map (sometimes also called the logistic map)*

$$x_{t+1} = 1 - ax_t^2, \tag{11.9}$$

*with the one critical point at  $x_c = 0$ . Further example is the repelling unimodal map of figure 11.8 (b).*

*Such dynamical systems are irreversible (the inverse of  $f$  is double-valued), but, as we shall show in sect. 12.2, they may nevertheless serve as effective descriptions of invertible 2-dimensional hyperbolic flows.*

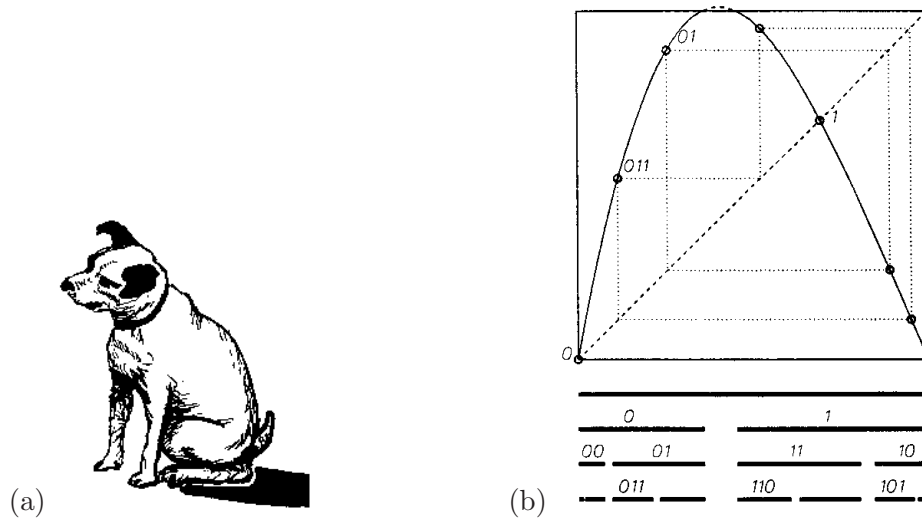


**Figure 11.8:** (a) The complete tent map together with intervals that follow the indicated itinerary for  $n$  steps. (b) A unimodal repeller with the remaining intervals after 1, 2 and 3 iterations. Intervals marked  $s_1 s_2 \dots s_n$  are unions of all points that do not escape in  $n$  iterations, and follow the itinerary  $S^+ = s_1 s_2 \dots s_n$ . Note that the spatial ordering does not respect the binary ordering; for example  $x_{00} < x_{01} < x_{11} < x_{10}$ . Also indicated: the fixed points  $x_0, x_1$ , the 2-cycle  $\overline{01}$ , and the 3-cycle  $\overline{011}$ .

For the unimodal maps of figure 11.8 a Markov partition of the unit interval  $\mathcal{M}$  is given by the two intervals  $\{\mathcal{M}_0, \mathcal{M}_1\}$ . We refer to (11.8) as the “complete” tent map because its symbolic dynamics is complete binary: as both  $f(\mathcal{M}_0)$  and  $f(\mathcal{M}_1)$  fully cover  $\mathcal{M}_0$  and  $\mathcal{M}_1$ , the corresponding transition matrix is a  $[2 \times 2]$  matrix with all entries equal to 1, as in (11.3). As binary symbolic dynamics pops up frequently in applications, we list the shortest binary prime cycles in table 11.1.

11.3  
page 182

The *critical value* denotes either the maximum or the minimum value of  $f(x)$  on the defining interval; we assume here that it is a maximum,  $f(x_c) \geq f(x)$  for all  $x \in \mathcal{M}$ . The critical value  $f(x_c)$  belongs neither to the left nor to the right partition  $\mathcal{M}_i$ , and is denoted by its own symbol  $s = C$ . As we shall see, its preimages serve as partition boundary points.

The trajectory  $x_1, x_2, x_3, \dots$  of the initial point  $x_0$  is given by the iteration  $x_{n+1} = f(x_n)$ . Iterating  $f$  and checking whether the point lands to the left or to the right of  $x_c$  generates a *temporally* ordered topological itinerary (11.17) for a given trajectory,

$$s_n = \begin{cases} 1 & \text{if } x_n > x_c \\ 0 & \text{if } x_n < x_c \end{cases} . \tag{11.10}$$

We shall refer to  $S^+(x_0) = .s_1 s_2 s_3 \dots$  as the *future itinerary*. Our next task is to answer the reverse problem: given an itinerary, what is the corresponding *spatial* ordering of points that belong to a given trajectory?

### 11.3.2 Spatial ordering, 1- $d$ maps

Suppose you have succeeded in constructing a covering symbolic dynamics, such as for a well-separated 3-disk system. Now start moving the disks toward each other. At some critical separation a disk will start blocking families of trajectories traversing the other two disks. The order in which trajectories disappear is determined by their relative ordering in space; the ones closest to the intervening disk will be pruned first. Determining inadmissible itineraries requires that we relate the spatial ordering of trajectories to their time ordered itineraries.

 12.9  
page 204

The easiest point of departure is to start out by working out this relation for the symbolic dynamics of 1-dimensional mappings. As it appears impossible to present this material without getting bogged down in a sea of 0's, 1's and subscripted subscripts, we announce the main result before embarking upon its derivation:

The admissibility criterion stated in sect. 11.4 eliminates *all* itineraries that cannot occur for a given unimodal map.

The tent map (11.8) consists of two straight segments joined at  $x = 1/2$ . The symbol  $s_n$  defined in (11.10) equals 0 if the function increases, and 1 if the function decreases. The piecewise linearity of the map makes it possible to analytically determine an initial point given its itinerary, a property that we now use to define a topological coordinatization common to all unimodal maps.

Here we have to face the fundamental problem of pedagogy: combinatorics cannot be taught. The best one can do is to state the answer, and then hope that you will figure it out by yourself. Once you figure it out, feel free to complain that the way the rule is stated here is incomprehensible. The tent map point  $\gamma(S^+)$  with future itinerary  $S^+$  is given by converting the sequence of  $s_n$ 's into a binary number by the following algorithm:

$$w_{n+1} = \begin{cases} w_n & \text{if } s_n = 0 \\ 1 - w_n & \text{if } s_n = 1 \end{cases}, \quad w_1 = s_1$$

$$\gamma(S^+) = 0.w_1w_2w_3 \dots = \sum_{n=1}^{\infty} w_n/2^n. \quad (11.11)$$

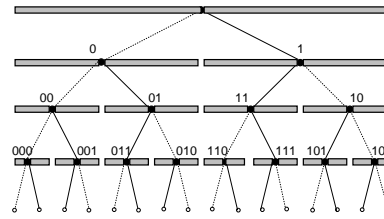
 11.6  
page 183

This follows by inspection from the binary tree of figure 11.9.

**Example 11.6 Converting  $\gamma$  to  $S^+$ :**  $\gamma$  whose itinerary is  $S^+ = 0110000 \dots$  is given by the binary number  $\gamma = .010000 \dots$ . Conversely, the itinerary of  $\gamma = .01$  is  $s_1 = 0$ ,  $f(\gamma) = .1 \rightarrow s_2 = 1$ ,  $f^2(\gamma) = f(.1) = 1 \rightarrow s_3 = 1$ , etc..

We shall refer to  $\gamma(S^+)$  as the (*future*) *topological coordinate*.  $w_t$ 's are the digits in the binary expansion of the starting point  $\gamma$  for the complete

**Figure 11.9:** Alternating binary tree relates the itinerary labeling of the unimodal map figure 11.8 intervals to their spatial ordering. Dotted line stands for 0, full line for 1; the binary sub-tree whose root is a full line (symbol 1) reverses the orientation, due to the orientation reversing fold in figures 11.7 and 11.8.



tent map (11.8). In the left half-interval the map  $f(x)$  acts by multiplication by 2, while in the right half-interval the map acts as a flip as well as multiplication by 2, reversing the ordering, and generating in the process the sequence of  $s_n$ 's from the binary digits  $w_n$ .

The mapping  $x_0 \rightarrow S^+(x_0) \rightarrow \gamma_0 = \gamma(S^+)$  is a *topological conjugacy* which maps the trajectory of an initial point  $x_0$  under iteration of a given unimodal map to that initial point  $\gamma$  for which the trajectory of the “canonical” unimodal map (11.8) has the same itinerary. The virtue of this conjugacy is that it *preserves the ordering* for any unimodal map in the sense that if  $\bar{x} > x$ , then  $\bar{\gamma} > \gamma$ .

## 11.4 Kneading theory

(K.T. Hansen and P. Cvitanović)

The main motivation for being mindful of spatial ordering of temporal itineraries is that this spatial ordering provides us with criteria that separate inadmissible orbits from those realizable by the dynamics. For 1-dimensional mappings the *kneading theory* provides such criterion of admissibility.

If the parameter in the quadratic map (11.9) is  $a > 2$ , then the iterates of the critical point  $x_c$  diverge for  $n \rightarrow \infty$ . As long as  $a \geq 2$ , any sequence  $S^+$  composed of letters  $s_i = \{0, 1\}$  is admissible, and any value of  $0 \leq \gamma < 1$  corresponds to an admissible orbit in the non-wandering set of the map. The corresponding repeller is a complete binary labeled Cantor set, the  $n \rightarrow \infty$  limit of the  $n$ th level covering intervals sketched in figure 11.8.

For  $a < 2$  only a subset of the points in the interval  $\gamma \in [0, 1]$  corresponds to admissible orbits. The forbidden symbolic values are determined by observing that the largest  $x_n$  value in an orbit  $x_1 \rightarrow x_2 \rightarrow x_3 \rightarrow \dots$  has to be smaller than or equal to the image of the critical point, *the critical value*  $f(x_c)$ . Let  $K = S^+(x_c)$  be the itinerary of the critical point  $x_c$ , denoted the *kneading sequence* of the map. The corresponding topological coordinate is called the *kneading value*

$$\kappa = \gamma(K) = \gamma(S^+(x_c)). \quad (11.12)$$



**Figure 11.10:** The “dike” map obtained by slicing of a top portion of the tent map figure 11.8 (a). Any orbit that visits the primary pruning interval  $(\kappa, 1]$  is inadmissible. The admissible orbits form the Cantor set obtained by removing from the unit interval the primary pruning interval and all its iterates. Any admissible orbit has the same topological coordinate and itinerary as the corresponding tent map figure 11.8 (a) orbit.

A map with the same kneading sequence  $K$  as  $f(x)$ , such as the dike map figure 11.10, is obtained by slicing off all  $\gamma(S^+(x_0)) > \kappa$ ,

$$f(\gamma) = \begin{cases} f_0(\gamma) = 2\gamma & \gamma \in I_0 = [0, \kappa/2) \\ f_c(\gamma) = \kappa & \gamma \in I_c = [\kappa/2, 1 - \kappa/2] \\ f_1(\gamma) = 2(1 - \gamma) & \gamma \in I_1 = [1 - \kappa/2, 1] \end{cases} . \quad (11.13)$$

The dike map is the complete tent map figure 11.8 (a) with the top sliced off. It is convenient for coding the symbolic dynamics, as those  $\gamma$  values that survive the pruning are the same as for the complete tent map figure 11.8 (a), and are easily converted into admissible itineraries by (11.11).

If  $\gamma(S^+) > \gamma(K)$ , the point  $x$  whose itinerary is  $S^+$  would exceed the critical value,  $x > f(x_c)$ , and hence cannot be an admissible orbit. Let

$$\hat{\gamma}(S^+) = \sup_m \gamma(\sigma^m(S^+)) \quad (11.14)$$

be the *maximal value*, the highest topological coordinate reached by the orbit  $x_1 \rightarrow x_2 \rightarrow x_3 \rightarrow \dots$ . We shall call the interval  $(\kappa, 1]$  the *primary pruned interval*. The orbit  $S^+$  is inadmissible if  $\gamma$  of any shifted sequence of  $S^+$  falls into this interval.

**Criterion of admissibility:** Let  $\kappa$  be the kneading value of the critical point, and  $\hat{\gamma}(S^+)$  be the maximal value of the orbit  $S^+$ . Then the orbit  $S^+$  is admissible if and only if  $\hat{\gamma}(S^+) \leq \kappa$ .

While a unimodal map may depend on many arbitrarily chosen parameters, its dynamics determines the unique kneading value  $\kappa$ . We shall call  $\kappa$  the *topological parameter* of the map. Unlike the parameters of the original dynamical system, the topological parameter has no reason to be either smooth or continuous. The jumps in  $\kappa$  as a function of the map parameter such as  $a$  in (11.9) correspond to inadmissible values of the topological parameter. Each jump in  $\kappa$  corresponds to a stability window associated with a stable cycle of a smooth unimodal map. For the quadratic map (11.9)  $\kappa$

increases monotonically with the parameter  $a$ , but for a general unimodal map such monotonicity need not hold.

For further details of unimodal dynamics, the reader is referred to appendix E.1. As we shall see in sect. 12.4, for higher dimensional maps and flows there is no single parameter that orders dynamics monotonically; as a matter of fact, there is an infinity of parameters that need adjustment for a given symbolic dynamics. This difficult subject is beyond our current ambition horizon.

## 11.5 Markov graphs

### 11.5.1 Finite memory

In the complete  $N$ -ary symbolic dynamics case (see example (11.3)) the choice of the next symbol requires no memory of the previous ones. However, any further refinement of the partition requires finite memory.

For example, for the binary labeled repeller with complete binary symbolic dynamics, we might chose to partition the phase space into four regions  $\{\mathcal{M}_{00}, \mathcal{M}_{01}, \mathcal{M}_{10}, \mathcal{M}_{11}\}$ , a 1-step refinement of the initial partition  $\{\mathcal{M}_0, \mathcal{M}_1\}$ . Such partitions are drawn in figure 11.4, as well as figure 1.9. Topologically  $f$  acts as a left shift (12.7), and its action on the rectangle  $.[01]$  is to move the decimal point to the right, to  $[0.1]$ , forget the past,  $.[1]$ , and land in either of the two rectangles  $\{.[10], [11]\}$ . Filling in the matrix elements for the other three initial states we obtain the 1-step memory transition matrix acting on the 4-state vector

$$\phi' = T\phi = \begin{pmatrix} T_{00,00} & 0 & T_{00,10} & 0 \\ T_{01,00} & 0 & T_{01,10} & 0 \\ 0 & T_{10,01} & 0 & T_{10,11} \\ 0 & T_{11,01} & 0 & T_{11,11} \end{pmatrix} \begin{pmatrix} \phi_{00} \\ \phi_{01} \\ \phi_{10} \\ \phi_{11} \end{pmatrix}. \quad (11.15)$$

 11.8  
page 183

By the same token, for  $M$ -step memory the only nonvanishing matrix elements are of the form  $T_{s_1 s_2 \dots s_{M+1}, s_0 s_1 \dots s_M}$ ,  $s_{M+1} \in \{0, 1\}$ . This is a sparse matrix, as the only non vanishing entries in the  $m = s_0 s_1 \dots s_M$  column of  $T_{dm}$  are in the rows  $d = s_1 \dots s_M 0$  and  $d = s_1 \dots s_M 1$ . If we increase the number of steps remembered, the transition matrix grows big quickly, as the  $N$ -ary dynamics with  $M$ -step memory requires an  $[N^{M+1} \times N^{M+1}]$  matrix. Since the matrix is very sparse, it pays to find a compact representation for  $T$ . Such representation is afforded by Markov graphs, which are not only compact, but also give us an intuitive picture of the topological dynamics.

 13.1  
page 226

Construction of a good Markov graph is, like combinatorics, unexplainable. The only way to learn is by some diagrammatic gymnastics, so we

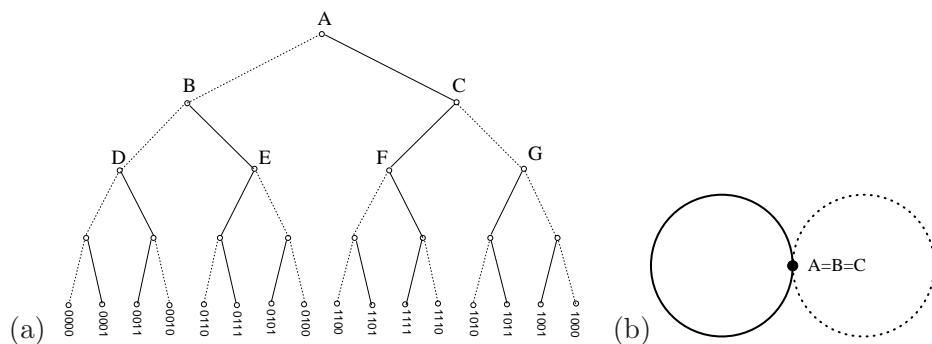


**Figure 11.11:** (a) The self-similarity of the complete binary symbolic dynamics represented by a binary tree (b) identification of nodes  $B = A$ ,  $C = A$  leads to the finite 1-node, 2-links Markov graph. All admissible itineraries are generated as walks on this finite Markov graph.

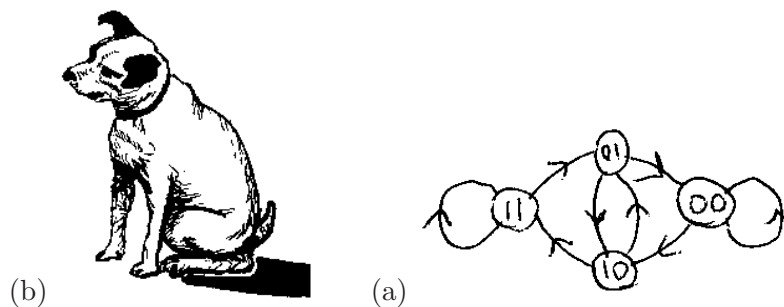


**Figure 11.12:** (a) The 2-step memory Markov graph, links version obtained by identifying nodes  $A = D = E = F = G$  in figure 11.11(a). Links of this graph correspond to the matrix entries in the transition matrix (11.15). (b) the 2-step memory Markov graph, node version.

work our way through a sequence of exercises in lieu of plethora of baffling definitions.

To start with, what do finite graphs have to do with infinitely long trajectories? To understand the main idea, let us construct a graph that enumerates all possible itineraries for the case of complete binary symbolic dynamics.

Mark a dot “.” on a piece of paper. Draw two short lines out of the dot, end each with a dot. The full line will signify that the first symbol in an itinerary is “1”, and the dotted line will signify “0”. Repeat the procedure for each of the two new dots, and then for the four dots, and so on. The result is the binary tree of figure 11.11(a). Starting at the top node, the tree enumerates exhaustively all distinct finite itineraries

$$\{0, 1\}, \{00, 01, 10, 11\}, \{000, 001, 010, \dots\}, \dots .$$

The  $M = 4$  nodes in figure 11.11(a) correspond to the 16 distinct binary strings of length 4, and so on. By habit we have drawn the tree as the alternating binary tree of figure 11.9, but that has no significance as far as enumeration of itineraries is concerned - an ordinary binary tree would serve just as well.

The trouble with an infinite tree is that it does not fit on a piece of paper. On the other hand, we are not doing much - at each node we are turning either left or right. Hence all nodes are equivalent, and can be identified. To say it in other words, the tree is self-similar; the trees originating in nodes  $B$  and  $C$  are themselves copies of the entire tree. The result of identifying  $B = A$ ,  $C = A$  is a single node, 2-link Markov graph of figure 11.11(b): any itinerary generated by the binary tree figure 11.11(a), no matter how long, corresponds to a walk on this graph.

This is the most compact encoding of the complete binary symbolic dynamics. Any number of more complicated Markov graphs can do the job as well, and might be sometimes preferable. For example, identifying the trees originating in  $D$ ,  $E$ ,  $F$  and  $G$  with the entire tree leads to the 2-step memory Markov graph of figure 11.12a. The corresponding transition matrix is given by (11.15).



in depth:  
chapter 12, p. 185



fast track:  
chapter 13, p. 205

## 11.6 Symbolic dynamics, basic notions

In this section we collect the basic notions and definitions of symbolic dynamics. The reader might prefer to skim through this material on first reading, return to it later as the need arises.

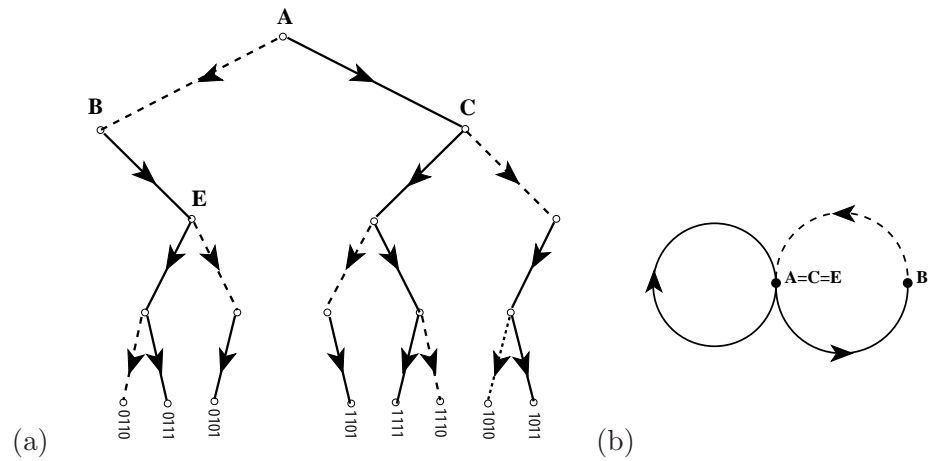


**Figure 11.13:** (a) The self-similarity of the  $\_00\_$ -pruned binary tree: trees originating from nodes  $C$  and  $E$  are the same as the entire tree. (b) Identification of nodes  $A = C = E$  leads to the finite 2-node, 3-links Markov graph; as 0 is always followed by 1, the walks on this graph generate only the admissible itineraries.

**Shifts.** We associate with every initial point  $x_0 \in \mathcal{M}$  the *future itinerary*, a sequence of symbols  $S^+(x_0) = s_1 s_2 s_3 \dots$  which indicates the order in which the regions are visited. If the trajectory  $x_1, x_2, x_3, \dots$  of the initial point  $x_0$  is generated by

$$x_{n+1} = f(x_n), \quad (11.16)$$

then the itinerary is given by the symbol sequence

$$s_n = s \quad \text{if} \quad x_n \in \mathcal{M}_s. \quad (11.17)$$

Similarly, the *past itinerary*  $S^-(x_0) = \dots s_{-2} s_{-1} s_0$  describes the history of  $x_0$ , the order in which the regions were visited before arriving to the point  $x_0$ . To each point  $x_0$  in the dynamical space we thus associate a bi-infinite itinerary

$$S(x_0) = (s_k)_{k \in \mathbb{Z}} = S^- \cdot S^+ = \dots s_{-2} s_{-1} s_0 \cdot s_1 s_2 s_3 \dots. \quad (11.18)$$

The itinerary will be finite for a scattering trajectory, entering and then escaping  $\mathcal{M}$  after a finite time, infinite for a trapped trajectory, and infinitely repeating for a periodic trajectory.

The set of all bi-infinite itineraries that can be formed from the letters of the alphabet  $\mathcal{A}$  is called the *full shift*

$$\mathcal{A}^{\mathbb{Z}} = \{(s_k)_{k \in \mathbb{Z}} : s_k \in \mathcal{A} \text{ for all } k \in \mathbb{Z}\}. \quad (11.19)$$

The jargon is not thrilling, but this is how professional dynamicists talk to each other. We will stick to plain English to the extent possible.

We refer to this set of all conceivable itineraries as the *covering* symbolic dynamics. The name *shift* is descriptive of the way the dynamics acts on these sequences. As is clear from the definition (11.17), a forward iteration  $x \rightarrow x' = f(x)$  shifts the entire itinerary to the left through the “decimal point”. This operation, denoted by the shift operator  $\sigma$ ,

$$\sigma(\cdots s_{-2}s_{-1}s_0.s_1s_2s_3\cdots) = \cdots s_{-2}s_{-1}s_0s_1.s_2s_3\cdots, \quad (11.20)$$

demoting the current partition label  $s_1$  from the future  $S^+$  to the “has been” itinerary  $S^-$ . The inverse shift  $\sigma^{-1}$  shifts the entire itinerary one step to the right.

A finite sequence  $b = s_k s_{k+1} \cdots s_{k+n_b-1}$  of symbols from  $\mathcal{A}$  is called a *block* of length  $n_b$ . A phase space trajectory is *periodic* if it returns to its initial point after a finite time; in the shift space the trajectory is periodic if its itinerary is an infinitely repeating block  $p^\infty$ . We shall refer to the set of periodic points that belong to a given periodic orbit as a *cycle*

$$p = \overline{s_1 s_2 \cdots s_{n_p}} = \{x_{s_1 s_2 \cdots s_{n_p}}, x_{s_2 \cdots s_{n_p} s_1}, \cdots, x_{s_{n_p} s_1 \cdots s_{n_p-1}}\}. \quad (11.21)$$

By its definition, a cycle is invariant under cyclic permutations of the symbols in the repeating block. A bar over a finite block of symbols denotes a periodic itinerary with infinitely repeating basic block; we shall omit the bar whenever it is clear from the context that the trajectory is periodic. Each *cycle point* is labeled by the first  $n_p$  steps of its future itinerary. For example, the 2nd cycle point is labeled by

$$x_{s_2 \cdots s_{n_p} s_1} = \overline{x_{s_2 \cdots s_{n_p} s_1} s_2 \cdots s_{n_p} s_1}.$$

A *prime cycle*  $p$  of length  $n_p$  is a single traversal of the orbit; its label is a block of  $n_p$  symbols that cannot be written as a repeat of a shorter block (in literature such cycle is sometimes called *primitive*; we shall refer to it as “prime” throughout this text).

**Partitions.** A partition is called *generating* if every infinite symbol sequence corresponds to a distinct point in the phase space. Finite Markov partition (11.4) is an example. Constructing a generating partition for a given system is a difficult problem. In examples to follow we shall concentrate on cases which allow finite partitions, but in practice almost any generating partition of interest is infinite.

A mapping  $f : \mathcal{M} \rightarrow \mathcal{M}$  together with a partition  $\mathcal{A}$  induces *topological dynamics*  $(\Sigma, \sigma)$ , where the *subshift*

$$\Sigma = \{(s_k)_{k \in \mathbb{Z}}\}, \quad (11.22)$$

is the set of all *admissible* infinite itineraries, and  $\sigma : \Sigma \rightarrow \Sigma$  is the shift operator (11.20). The designation “subshift” comes from the fact that

$\Sigma \subset \mathcal{A}^{\mathbb{Z}}$  is the subset of the full shift (11.19). One of our principal tasks in developing symbolic dynamics of dynamical systems that occur in nature will be to determine  $\Sigma$ , the set of all bi-infinite itineraries  $S$  that are actually realized by the given dynamical system.

A partition too coarse, coarser than, for example, a Markov partition, would assign the same symbol sequence to distinct dynamical trajectories. To avoid that, we often find it convenient to work with partitions finer than strictly necessary. Ideally the dynamics in the refined partition assigns a unique infinite itinerary  $\cdots s_{-2}s_{-1}s_0.s_1s_2s_3\cdots$  to each distinct trajectory, but there might exist full shift symbol sequences (11.19) which are not realized as trajectories; such sequences are called *inadmissible*, and we say that the symbolic dynamics is *pruned*. The word is suggested by “pruning” of branches corresponding to forbidden sequences for symbolic dynamics organized hierarchically into a tree structure, as explained in sect. 11.5.

**Pruning.** If the dynamics is pruned, the alphabet must be supplemented by a *grammar*, a set of pruning rules. After the inadmissible sequences have been pruned, it is often convenient to parse the symbolic strings into words of variable length - this is called *coding*. Suppose that the grammar can be stated as a finite number of pruning rules, each forbidding a block of finite length,

$$\mathcal{G} = \{b_1, b_2, \cdots b_k\}, \quad (11.23)$$

where a *pruning block*  $b$  is a sequence of symbols  $b = s_1s_2\cdots s_{n_b}$ ,  $s \in \mathcal{A}$ , of finite length  $n_b$ . In this case we can always construct a finite Markov partition (11.4) by replacing finite length words of the original partition by letters of a new alphabet. In particular, if the longest forbidden block is of length  $M + 1$ , we say that the symbolic dynamics is a shift of finite type with  $M$ -step memory. In that case we can *recode* the symbolic dynamics in terms of a new alphabet, with each new letter given by an admissible block of at most length  $M$ . In the new alphabet the grammar rules are implemented by setting  $T_{ij} = 0$  in (11.3) for forbidden transitions.

A topological dynamical system  $(\Sigma, \sigma)$  for which all admissible itineraries are generated by a finite transition matrix

$$\Sigma = \{(s_k)_{k \in \mathbb{Z}} : T_{s_k s_{k+1}} = 1 \text{ for all } k\} \quad (11.24)$$

is called a subshift of *finite type*. Such systems are particularly easy to handle; the topology can be converted into symbolic dynamics by representing the transition matrix by a finite directed *Markov graph*, a convenient visualization of topological dynamics.

**Markov graphs.** A Markov graph describes compactly the ways in which the phase-space regions map into each other, accounts for finite memory effects in dynamics, and generates the totality of admissible trajectories as the set of all possible walks along its links.

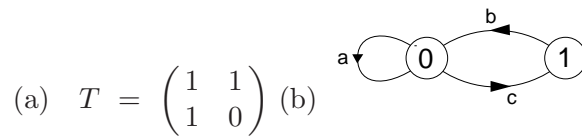


**Figure 11.14:** (a) The transition matrix for a simple subshift on two-state partition  $\mathcal{A} = \{0, 1\}$ , with grammar  $\mathcal{G}$  given by a single pruning block  $b = 11$  (consecutive repeat of symbol 1 is inadmissible): the state  $\mathcal{M}_0$  maps both onto  $\mathcal{M}_0$  and  $\mathcal{M}_1$ , but the state  $\mathcal{M}_1$  maps only onto  $\mathcal{M}_0$ . (b) The corresponding finite 2-node, 3-links Markov graph, with nodes coding the symbols. All admissible itineraries are generated as walks on this finite Markov graph.

A Markov graph consists of a set of *nodes* (or *vertices*, or *states*), one for each state in the alphabet  $\mathcal{A} = \{A, B, C, \dots, Z\}$ , connected by a set of directed *links* (*edges*, *arcs*). Node  $i$  is connected by a directed link to node  $j$  whenever the transition matrix element (11.2) takes value  $T_{ij} = 1$ . There might be a set of links connecting two nodes, or links that originate and terminate on the same node. Two graphs are isomorphic if one can be obtained from the other by relabeling links and nodes; for us they are one and the same graph. As we are interested in recurrent dynamics, we restrict our attention to *irreducible* or *strongly connected* graphs, i.e., graphs for which there is a path from any node to any other node.

The simplest example is given in figure 11.14.



in depth:  
chapter 12, p. 185

## Commentary

**Remark 11.1** Symbolic dynamics, history and good taste. For a brief history of symbolic dynamics, from J. Hadamard in 1898 onward, see Notes to chapter 1 of Kitchens monograph [11.1], a very clear and enjoyable mathematical introduction to topics discussed here. Finite Markov graphs or finite automata are discussed in refs. [11.2, 11.3, 11.4, 11.5]. They belong to the category of regular languages. A good hands-on introduction to symbolic dynamics is given in ref. [11.6].

The binary labeling of the once-folding map periodic points was introduced by Myrberg [11.7] for one-dimensional maps, and its utility to two-dimensional maps has been emphasized in refs. [3.7, 3.11]. For one-dimensional maps it is now customary to use the *R-L* notation of Metropolis, Stein and Stein [11.8, 11.9], indicating that the point  $x_n$  lies either to the left or to the right of the critical point in figure 11.8. The symbolic dynamics of such mappings has been extensively studied by means of the Smale horseshoes, see for example ref. [11.10]. Using letters rather than numerals in symbol dynamics alphabets probably reflects good taste. We prefer numerals for their computational convenience, as they speed up the implementation of conversions into the topological coordinates  $(\delta, \gamma)$  introduced in sect. 12.3.1. The alternating binary ordering of figure 11.9 is related to the Gray codes of computer science [2.8].

**Remark 11.2** Inflating Markov graphs. In the above examples the symbolic dynamics has been encoded by labeling links in the Markov graph. Alternatively one can encode the dynamics by labeling the nodes, as in figure 11.12, where the 4 nodes refer to 4 Markov partition regions  $\{\mathcal{M}_{00}, \mathcal{M}_{01}, \mathcal{M}_{10}, \mathcal{M}_{11}\}$ , and the 8 links to the 8 non-zero entries in the 2-step memory transition matrix (11.15).

## Résumé

In chapters 14 and 15 we will establish that spectra of evolution operators can be extracted from periodic orbit sums:

$$\sum (\text{spectral eigenvalues}) = \sum (\text{periodic orbits}) .$$

In order to implement this theory we need to know what periodic orbits can exist, and the symbolic dynamics developed above and in chapter 12 is an invaluable tool toward this end.



fast track:  
chapter 13, p. 205

## References

- [11.1] B.P. Kitchens, *Symbolic dynamics: one-sided, two-sided, and countable state Markov shifts* (Springer, Berlin 1998).
- [11.2] A. Salomaa, *Formal Languages* (Academic Press, San Diego, 1973).
- [11.3] J.E. Hopcroft and J.D. Ullman, *Introduction to Automata Theory, Languages, and Computation* (Addison-Wesley, Reading MA, 1979).
- [11.4] D.M. Cvetković, M. Doob and H. Sachs, *Spectra of Graphs* (Academic Press, New York, 1980).
- [11.5] P. Grassberger, “On the symbolic dynamics of the one-humped map of the interval” *Z. Naturforsch. A* **43**, 671 (1988).
- [11.6] D.A. Lind and B. Marcus, *An introduction to symbolic dynamics and coding* (Cambridge Univ. Press, Cambridge 1995).
- [11.7] P.J. Myrberg, *Ann. Acad. Sc. Fenn., Ser. A*, **256**, 1 (1958); **259**, 1 (1958).
- [11.8] N. Metropolis, M.L. Stein and P.R. Stein, “On Finite Limit Sets for Transformations on the Unit Interval”, *J. Comb. Theo.* **15**, 25 (1973).
- [11.9] P. Collet and J.P. Eckmann, *Iterated Maps on the Interval as Dynamical Systems* (Birkhauser, Boston, 1980).
- [11.10] J. Guckenheimer and P. Holmes, *Non-linear Oscillations, Dynamical Systems and Bifurcations of Vector Fields* (Springer, New York, 1986).

- [11.11] R.L. Devaney, *An Introduction to Chaotic Dynamical Systems* (Addison-Wesley, Reading MA, 1987).
- [11.12] R.L. Devaney, *A First Course in Chaotic Dynamical Systems* (Addison-Wesley, Reading MA, 1992).
- [11.13] Bai-Lin Hao, *Elementary symbolic dynamics and chaos in dissipative systems* (World Scientific, Singapore, 1989).
- [11.14] E. Aurell, “Convergence of dynamical zeta functions”, *J. Stat. Phys.* **58**, 967 (1990).
- [11.15] M.J. Feigenbaum, *J. Stat. Phys.* **46**, 919 (1987); **46**, 925 (1987).
- [11.16] P. Cvitanović, “Chaos for cyclists”, in E. Moss, ed., *Noise and chaos in nonlinear dynamical systems* (Cambridge Univ. Press, Cambridge 1989).
- [11.17] P. Cvitanović, “The power of chaos”, in J.H. Kim and J. Stringer, eds., *Applied Chaos*, (John Wiley & Sons, New York 1992).
- [11.18] P. Cvitanović, ed., *Periodic Orbit Theory - theme issue, CHAOS* **2**, 1-158 (1992).
- [11.19] P. Cvitanović, “Dynamical averaging in terms of periodic orbits”, *Physica D* **83**, 109 (1995).